



Natural convection of non-Newtonian power-law fluids on a horizontal plate



Abhijit Guha*, Kaustav Pradhan

Mechanical Engineering Department, Indian Institute of Technology Kharagpur, Kharagpur 721302, India

ARTICLE INFO

Article history:

Received 15 August 2013

Received in revised form 8 October 2013

Accepted 1 November 2013

Keywords:

Natural convection

Non-Newtonian

Horizontal plate

ABSTRACT

The problem of natural convective boundary layer flow of a non-Newtonian power-law fluid over an isothermal horizontal plate, which does not admit a similarity solution, has been solved numerically using a time-marching finite difference method. The analysis shows that the velocity, temperature and pressure inside the boundary layer depend on two parameters, the non-Newtonian power-law index (n) and the generalised Prandtl number (Pr^*). For $n > 1$ (dilatant fluids), the u -velocity profiles reveal that the maximum velocity attained increases but the thickness of the boundary layer decreases as the value of n is progressively increased above unity. For $n < 1$ (pseudoplastic fluids), the reverse occurs and the boundary layer thickness increases to a great extent while the maximum velocity is reduced as the value of n is progressively decreased below unity. The magnitude of the normal velocity component at the edge of the boundary layer is found to be smaller for dilatant fluids and larger for pseudoplastic fluids as compared to Newtonian fluids. It has been found that the dilatant fluids show improved heat transfer characteristics as compared to Newtonian and pseudoplastic fluids at the same generalised Prandtl number. The non-existence of self-similar solutions for non-Newtonian power-law fluids has been established, thus showing the utility of the numerical method developed to solve the system of partial differential equations.

© 2013 Elsevier Ltd. All rights reserved.

1. Introduction

Natural convection flow is driven by buoyancy forces generated by density differences that can be caused by temperature gradients in the fluid. Natural convection is commonly encountered in processes like cooling of electronic equipments, nuclear reactors, solar devices, in polymer processing industries, food industries, etc. [1–4].

The present paper deals with natural convection of non-Newtonian fluids on horizontal surfaces. Natural convection from vertical plates has been explored extensively. In comparison, the number of studies on natural convection from horizontal surfaces is rather limited. In case of a heated vertical plate, as the hotter fluid moves up, colder fluid comes in from the surrounding, principally in the horizontal direction. In case of a heated horizontal plate facing upward, on the other hand, the buoyancy force gives rise to a pressure gradient perpendicular to the plate which in turn results in a pressure gradient along the plate. It is the latter that drives the natural convective flow. Thus there is a significant difference between the flow physics of natural convection on vertical and horizontal surfaces. Unlike the boundary layer that forms due to forced

convection, the boundary layer on a horizontal plate due to natural convection is such that $\partial p/\partial y \neq 0$ and $\partial p/\partial x$ cannot be neglected inside the boundary layer (even when $\partial p_\infty/\partial x$ is zero). Several of such subtle physics of natural convection above a horizontal plate have been included in the theory formulated in this paper.

Having explained the distinguishing features of horizontal surfaces, we turn our attention to the other important feature of the present paper that is the fluid is non-Newtonian in nature. The study of heat transfer in non-Newtonian fluids has gained much importance due to a large number of industries (food processing, heat exchanger and reactor cooling, biochemical processes, etc.) dealing with these types of fluids [5–7]. The boundary layer flow of non-Newtonian fluids exhibits characters different from that of the conventional Newtonian fluids due to the non-linear variation of the shear stress with strain rate. There are several models to describe non-Newtonian fluid behaviour [8]. The power-law model [8] has been used widely to describe the flow of non-Newtonian fluids, in which the viscosity is assumed to vary as follows:

$$\mu = \mu_0 \left| \frac{\partial u}{\partial y} \right|^{n-1} \quad (1)$$

where n is the power-law index, constant for a particular fluid. Depending on the value of n , fluids are classified into three broad

* Corresponding author.

E-mail address: a.guha@mech.iitkgp.ernet.in (A. Guha).

$$\mu = \mu_0 \left| \frac{\partial u}{\partial y} \right|^{n-1} \tag{6}$$

The boundary conditions are

$$\text{at } y = 0, \quad u = 0, \quad v = 0, \quad T = T_w \tag{7}$$

$$\text{as } y \rightarrow \infty, \quad u \rightarrow 0, \quad T \rightarrow T_\infty, \quad p \rightarrow p_\infty \tag{8}$$

$$\text{at } x = 0, \quad u = 0, \quad v = 0, \quad T = T_\infty. \tag{9}$$

Here, u and v are the components of velocity along the x and y axes respectively, T is the local temperature of the fluid, μ_0 is the base viscosity of the fluid, g is the magnitude of the acceleration due to gravity, β is the co-efficient of volume expansion of the fluid, α is the thermal diffusivity, ρ is the density of the fluid, c_p is the specific heat capacity of the fluid and n is the power-law index for the non-Newtonian fluid.

Following an order of magnitude analysis (Appendix), Eqs. (2)–(9) are non-dimensionalized by using the definitions given below:

$$\bar{x} = \frac{x}{L}, \quad \bar{y} = \frac{y}{L} (Gr^*)^{1/(2n+3)}, \quad \bar{u} = \frac{u}{u_0}, \quad \bar{v} = \frac{v}{u_0} (Gr^*)^{1/(2n+3)},$$

$$\bar{p} = \frac{p - p_\infty}{\rho u_0^2}, \quad \theta = \frac{T - T_\infty}{T_w - T_\infty} \tag{10}$$

where the scaling velocity is given by

$$u_0 = \frac{v_0}{L} (Gr^*)^{(n+1)/(2n+3)} \tag{11}$$

The derivation of the appropriate velocity scale and length scale for the y -direction is given in the Appendix.

The dimensionless parameters are defined as follows:

$$Re^* = \frac{\rho u_0^{2-n} L^n}{\mu_0},$$

$$Gr^* = \frac{\{g\beta(T_w - T_\infty)\}^{(2n+3)/(2n^2+2n+1)} L^{(8n^2+10n-3)/(2n^2+2n+1)}}{v_0^{(4n^2+6n)/(2n^2+2n+1)}} \tag{12a}$$

$$Re = \frac{\rho u_0 L}{\mu_0}, \quad Gr = \frac{g\beta(T_w - T_\infty)L^3}{v_0^2}, \quad Pr = \frac{v_0}{\alpha}, \quad Ec = \frac{u_0^2}{c_p(T_w - T_\infty)} \tag{12b}$$

It can be observed from Eqs. (12a) and (12b) that the expressions for the generalised Reynolds number and the generalised Grashof number reduce to those of the Reynolds number and Grashof number for Newtonian fluids when $n = 1$.

Substitution of the non-dimensional variables defined in Eq. (10) into Eqs. (2)–(9) leads to the following non-dimensional equations:

$$\frac{\partial \bar{u}}{\partial \bar{x}} + \frac{\partial \bar{v}}{\partial \bar{y}} = 0 \tag{13}$$

$$\bar{u} \frac{\partial \bar{u}}{\partial \bar{x}} + \bar{v} \frac{\partial \bar{u}}{\partial \bar{y}} = -\frac{\partial \bar{p}}{\partial \bar{x}} + \frac{\partial}{\partial \bar{y}} \left(\left| \frac{\partial \bar{u}}{\partial \bar{y}} \right|^{n-1} \frac{\partial \bar{u}}{\partial \bar{y}} \right) \tag{14}$$

$$0 = -\frac{\partial \bar{p}}{\partial \bar{y}} + \theta \tag{15}$$

$$\bar{u} \frac{\partial \theta}{\partial \bar{x}} + \bar{v} \frac{\partial \theta}{\partial \bar{y}} = \frac{1}{Pr^*} \frac{\partial^2 \theta}{\partial \bar{y}^2} + Ec \left| \frac{\partial \bar{u}}{\partial \bar{y}} \right|^{(n-1)} \left(\frac{\partial \bar{u}}{\partial \bar{y}} \right)^2 \tag{16}$$

subject to the boundary conditions

$$\text{at } \bar{y} = 0, \quad \bar{u} = \bar{v} = 0, \quad \theta = 1 \tag{17}$$

$$\text{as } \bar{y} \rightarrow \infty, \quad \bar{u} \rightarrow 0, \quad \theta \rightarrow 0, \quad \bar{p} \rightarrow 0 \tag{18}$$

$$\text{at } \bar{x} = 0, \quad \bar{u} = \bar{v} = 0, \quad \theta = 0 \tag{19}$$

The specific heat capacity c_p of power-law fluids is of the order of 10^3 J/kg K. In natural convection, a typical value of the temperature difference between the heated plate and ambient fluid ($T_w - T_\infty$) may be of the order of 10^1 K; the scaling velocity u_0 would then be of the order of 10^{-1} m/s, The Eckert number (Ec) given in Eq. (12b) turns out to be very small ($\sim 10^{-6}$). Hence, the viscous dissipation term in Eq. (16) can be neglected.

$$\bar{u} \frac{\partial \theta}{\partial \bar{x}} + \bar{v} \frac{\partial \theta}{\partial \bar{y}} = \frac{1}{Pr^*} \frac{\partial^2 \theta}{\partial \bar{y}^2} \tag{20}$$

The two parameters appearing in the above system of Eqs. (13)–(15) and (20) are the power-law index n and the generalised Prandtl number Pr^* , the former having been defined in Eq. (1) and the latter defined as

$$Pr^* = \frac{u_0 L}{\alpha} (Re^*)^{-2/(n+1)} = Pr Re (Re^*)^{-2/(n+1)} \tag{21}$$

Using the results of the order of magnitude analysis (Appendix) and the expression for the scaling velocity given in Eq. (11), the generalised Prandtl number can be related to the Prandtl number as follows:

$$Pr^* = Pr (Gr^*)^{(n-1)/(2n+3)} \tag{22}$$

Of particular interest in our analysis, are the local heat transfer coefficient and the local skin friction coefficient.

Using Eqs. (1), (10), and (11), the wall shear stress and the surface heat flux can be expressed as:

$$\tau_w = \left(\mu_0 \left(\frac{\partial u}{\partial y} \right)^n \right)_{y=0} = \mu_0 \left(\frac{u_0}{L} \right)^n (Gr^*)^{n/(2n+3)} \left(\left(\frac{\partial \bar{u}}{\partial \bar{y}} \right)^n \right)_{\bar{y}=0} \tag{23}$$

$$q_w = -k \left(\frac{\partial T}{\partial y} \right)_{y=0} = -\frac{k(T_w - T_\infty)}{L} (Gr^*)^{1/(2n+3)} \left(\frac{\partial \theta}{\partial \bar{y}} \right)_{\bar{y}=0} \tag{24}$$

The skin-friction coefficient and the heat transfer coefficient can be calculated from Eqs. (23) and (24) as follows:

$$c_f = \frac{\tau_w}{\frac{1}{2} \rho u_0^2} = 2 (Gr^*)^{-1/(2n+3)} \left(\left(\frac{\partial \bar{u}}{\partial \bar{y}} \right)^n \right)_{\bar{y}=0} \tag{25}$$

$$h = \frac{q_w}{(T_w - T_\infty)} = -\frac{k}{L} (Gr^*)^{1/(2n+3)} \left(\frac{\partial \theta}{\partial \bar{y}} \right)_{\bar{y}=0} \tag{26}$$

The reduced skin-friction coefficient and reduced Nusselt number are given by:

$$c_f^* = \frac{c_f}{2 (Gr^*)^{-1/(2n+3)}} = \left(\left(\frac{\partial \bar{u}}{\partial \bar{y}} \right)^n \right)_{\bar{y}=0} \tag{27}$$

$$Nu^* = \frac{Nu}{(Gr^*)^{1/(2n+3)}} = \frac{hL/k}{(Gr^*)^{1/(2n+3)}} = -\left(\frac{\partial \theta}{\partial \bar{y}} \right)_{\bar{y}=0} \tag{28}$$

2.1. Search for a similarity solution

Natural convection boundary layer flow of Newtonian fluids on horizontal surfaces admit self-similar solutions [12,13]. In this section the existence (or non-existence) of self-similar solutions for non-Newtonian fluids exhibiting power-law variation in viscosity and constancy in thermal conductivity [14,19] is investigated.

A dimensionless stream function ψ defined by

$$\bar{u} = \frac{\partial \psi}{\partial \bar{y}} \quad \text{and} \quad \bar{v} = -\frac{\partial \psi}{\partial \bar{x}} \tag{29}$$

is introduced which automatically satisfies the continuity equation.

The non-dimensional boundary layer Eqs. (13)–(15) and (20) can then be represented in terms of ψ , \bar{p} and θ along with the corresponding boundary conditions. For finding the similarity variable, the generalised stretching transformation is applied and the different variables are stretched as follows:

$$\psi^* = c_1\psi, \quad \bar{x}^* = c_2\bar{x}, \quad \bar{y}^* = c_3\bar{y}, \quad \theta^* = c_4\theta, \quad \bar{p}^* = c_5\bar{p} \quad (30)$$

where c_1, c_2, c_3, c_4 and c_5 are arbitrary positive constants. Using the above, the stretched boundary layer equations take the form:

$$\frac{c_2 c_3^2}{c_1^2} \left(\frac{\partial \psi^*}{\partial \bar{y}^*} \frac{\partial^2 \psi^*}{\partial \bar{x}^* \partial \bar{y}^*} - \frac{\partial \psi^*}{\partial \bar{x}^*} \frac{\partial^2 \psi^*}{\partial \bar{y}^{*2}} \right) = -\frac{c_2}{c_5} \frac{\partial \bar{p}^*}{\partial \bar{x}^*} + \frac{c_3^{2n+1}}{c_1^n} \frac{\partial}{\partial \bar{y}^*} \left(\left| \frac{\partial^2 \psi^*}{\partial \bar{y}^{*2}} \right|^{n-1} \frac{\partial^2 \psi^*}{\partial \bar{y}^{*2}} \right) \quad (31)$$

$$0 = -\frac{c_3}{c_5} \frac{\partial \bar{p}^*}{\partial \bar{y}^*} + \frac{1}{c_4} \theta^* \quad (32)$$

$$\frac{c_2 c_3}{c_1 c_4} \left(\frac{\partial \psi^*}{\partial \bar{y}^*} \frac{\partial \theta^*}{\partial \bar{x}^*} - \frac{\partial \psi^*}{\partial \bar{x}^*} \frac{\partial \theta^*}{\partial \bar{y}^*} \right) = \frac{1}{Pr^*} \frac{c_3^2}{c_4} \frac{\partial^2 \theta^*}{\partial \bar{y}^{*2}} \quad (33)$$

The corresponding boundary conditions are as follows:

$$\text{at } \bar{y}^* = 0, \quad \frac{\partial \psi^*}{\partial \bar{y}^*} = \frac{\partial \psi^*}{\partial \bar{x}^*} = 0, \quad \frac{1}{c_4} \theta^* = 1 \quad (34)$$

$$\text{as } \bar{y}^* \rightarrow \infty, \quad \frac{\partial \psi^*}{\partial \bar{y}^*} \rightarrow 0, \quad \theta^* \rightarrow 0, \quad \bar{p}^* \rightarrow 0 \quad (35)$$

$$\text{at } \bar{x}^* = 0, \quad \frac{\partial \psi^*}{\partial \bar{y}^*} = \frac{\partial \psi^*}{\partial \bar{x}^*} = 0, \quad \theta^* = 0 \quad (36)$$

The boundary layer equations along with their boundary conditions should remain invariant under the stretching transformation. Hence from Eqs. (31), (32), and (34):

$$c_3^2 = \frac{c_1^2}{c_5}, \quad \frac{c_2 c_3^2}{c_1^2} = \frac{c_3^{2n+1}}{c_1^n}, \quad c_5 = c_3 c_4, \quad c_4 = 1 \quad (37)$$

Re-arranging the above equations, the expressions for the constants in terms of c_3 are as follows:

$$c_5 = c_3, \quad c_1 = c_3^{3/2}, \quad c_2 = c_3^{(n+4)/2} \quad (38)$$

Putting the values of the constants obtained above into the energy Eq. (33) gives the relation

$$c_2^{(n+3)/2} = c_2^2 \quad (39)$$

This is true if and only if $n = 1$. So we get consistent values of the arbitrary constants and hence a similarity variable only for $n = 1$ (Newtonian fluid). Hence, it can be stated that self-similar solutions do not exist for non-Newtonian power-law fluids with the adopted specification of viscosity and thermal conductivity. Keeping this in mind we proceed towards devising a method to solve the system of partial differential equations directly without resorting to any kind of transformations.

3. Method of numerical solution

The computation is challenging since one has to overcome several sources of convective numerical instability due to the basic non-linear nature of the governing partial differential equations. The present problem is more difficult than solving forced convection on a horizontal plate (for which there is an imposed velocity and $\partial p/\partial y$ is zero) or than solving natural convection on a vertical surface (for which $\partial p/\partial y$ is zero and $\partial p/\partial x$ does not appear in the final equation). The existence of the highly non-linear viscous

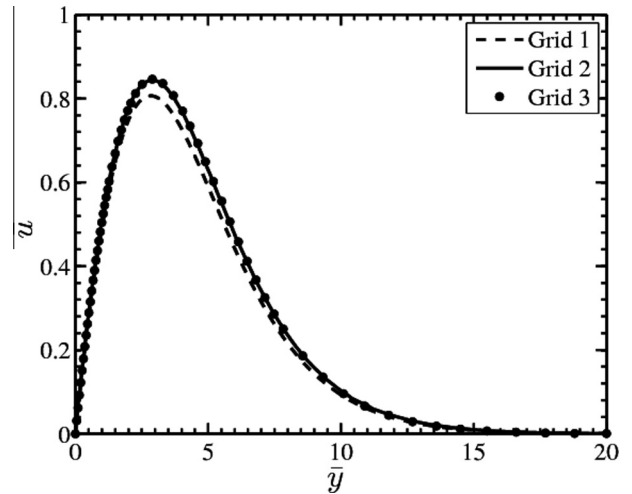


Fig. 1. Results of the grid independence test performed for three different grids for $n = 1$ and $Pr^* = 1$ at $\bar{x} = 5$.

Table 1

Comparison of the reduced skin-friction coefficient and reduced Nusselt number with published results for $n = 1, Pr^* = 1$ at $\bar{x} = 5$.

	Reduced skin-friction coefficient (c_f)	Reduced Nusselt number (Nu^*)
Rotem and Claassen [12]	0.6277	0.2060
Samanta and Guha [13]	0.6243	0.2046
Present work	0.6253	0.2091

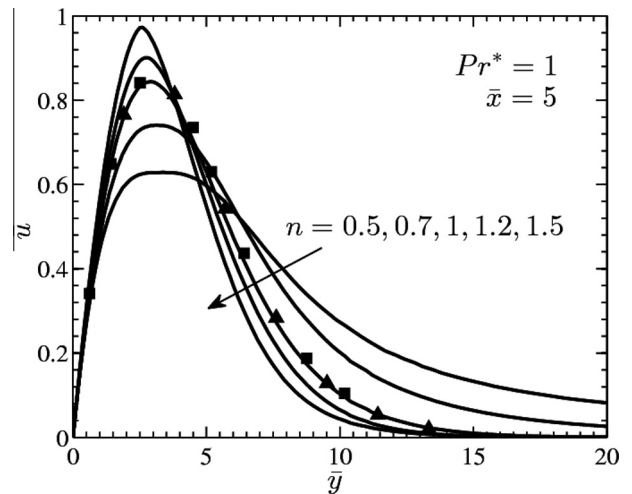


Fig. 2. Variation of non-dimensional u -velocity inside the boundary layer for different values of the non-Newtonian parameter for $Pr^* = 1$ at $\bar{x} = 5$. Keys: ■ Rotem and Claassen [12], ▲ Samanta and Guha [13], — Present work. [The y axis is shown here up to a value of 20 for clarity of the graphs, the maximum value used in the computation is far greater to ensure \bar{u} asymptotically approaches zero.]

stress term also gives rise to additional complexity as compared to the numerical simulation for Newtonian fluids.

Eqs. (13)–(15) and (20), subject to the boundary conditions (17)–(19), represent a set of coupled, non-linear partial differential equations. An in-house computer program has been written to solve these equations using the explicit finite difference scheme. A non-uniform grid is used in the \bar{y} -direction while a uniform grid is used for the distance \bar{x} along the plate. Three grid arrangements are used to check the grid independence of the solution for the case

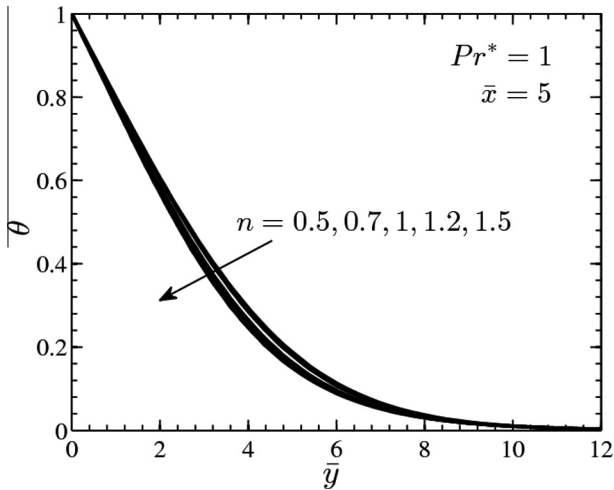


Fig. 3. Variation of non-dimensional temperature inside the boundary layer for different values of the non-Newtonian parameter for $Pr^* = 1$ at $\bar{x} = 5$.

of $n = 1$ and $Pr^* = 1$; Grid 1 (18×60), Grid 2 (35×120) and Grid 3 (60×230). It is found that, out of all flow variables, the u -velocity profiles show the maximum variation as the grid size is altered. This is why the u -velocity profiles are plotted in Fig. 1 in order to ascertain that grid independence is achieved. Based on such considerations, Grid 2 has been used for the example computations presented in this paper.

The values of the skin friction coefficient and Nusselt number depend strongly on the size of the first computational cell (Δy_1) at the solid surface. A reduction of this size improves accuracy but requires more computational time for convergence. From numerical experiments, a value of $\Delta y_1 = 0.05$ is selected; the subsequent grid sizes in the \bar{y} direction are increased according to a geometric progression series.

It is found during the present course of research that the choice of the size of the computational domain is very important and should be chosen so as to ensure that the velocity, pressure and temperature inside the boundary layer reach the ambient conditions asymptotically. For example, at $Pr^* = 1$, for Newtonian ($n = 1$) and dilatant ($n > 1$) fluids the maximum value of \bar{y} is taken as 20; for $n = 0.7$, maximum \bar{y} is taken as 50; for $n = 0.5$, maximum \bar{y} is taken as 220. These values are used to ensure that

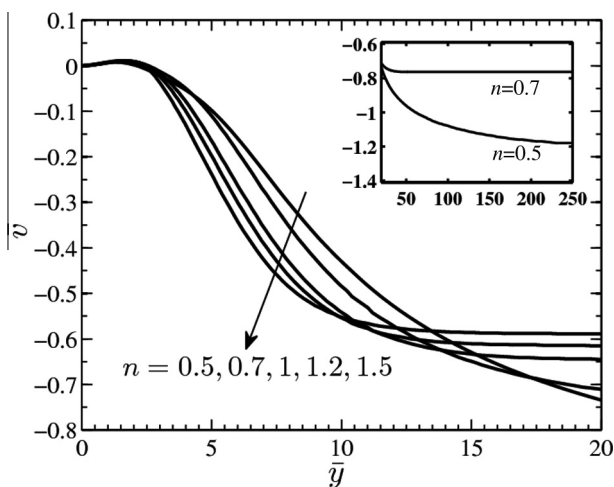


Fig. 4. Variation of non-dimensional v -velocity inside the boundary layer for different values of the non-Newtonian parameter for $Pr^* = 1$ at $\bar{x} = 5$.

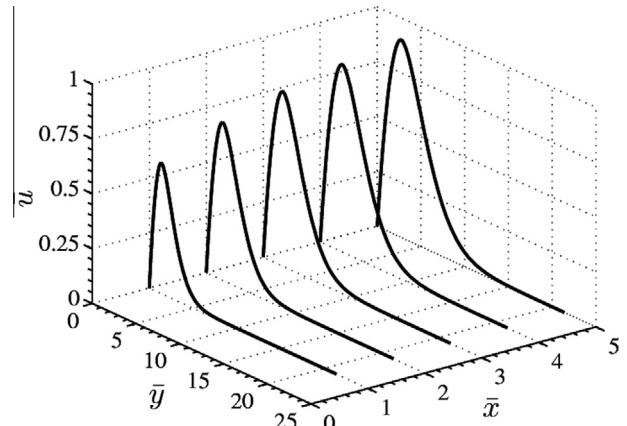


Fig. 5. Variation of non-dimensional u -velocity inside the boundary layer at different locations along the plate for a non-Newtonian fluid of $n = 1.2$ and $Pr^* = 1$.

$\bar{u} \leq 10^{-4}$ at the boundary of the computational domain for all computations.

It is evident from Eq. (1) that the effective viscosity depends on the inverse of the velocity gradient for shear-thinning fluids. Therefore, numerical difficulty is encountered in calculating the effective viscosity where the velocity gradient approaches zero (at the point of maximum velocity and at the edge of the boundary layer). To circumvent this difficulty, a lower limit (10^{-5}) of the velocity gradient is set for the evaluation of the coefficient of viscosity: if $|\partial \bar{u} / \partial \bar{y}| \geq 10^{-5}$, then Eq. (1) is used; if $|\partial \bar{u} / \partial \bar{y}| < 10^{-5}$, then $|\partial \bar{u} / \partial \bar{y}| = 10^{-5}$ is used while evaluating the viscosity.

Table 1 shows that the values of the Nusselt number and the skin-friction coefficient determined by the computer program developed for the present work match well with those calculated by similarity theory [12,13] for a Newtonian fluid. Fig. 2 provides a comparison of the u -velocity profile for a Newtonian fluid predicted by the present method and that calculated by similarity theory [12,13].

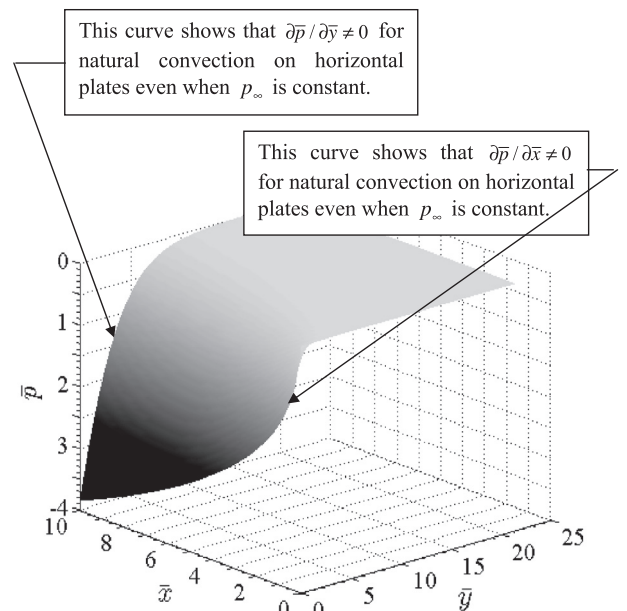


Fig. 6. Spatial variation of non-dimensional pressure inside the boundary layer for a non-Newtonian fluid of $n = 1.2$ and $Pr^* = 1$.

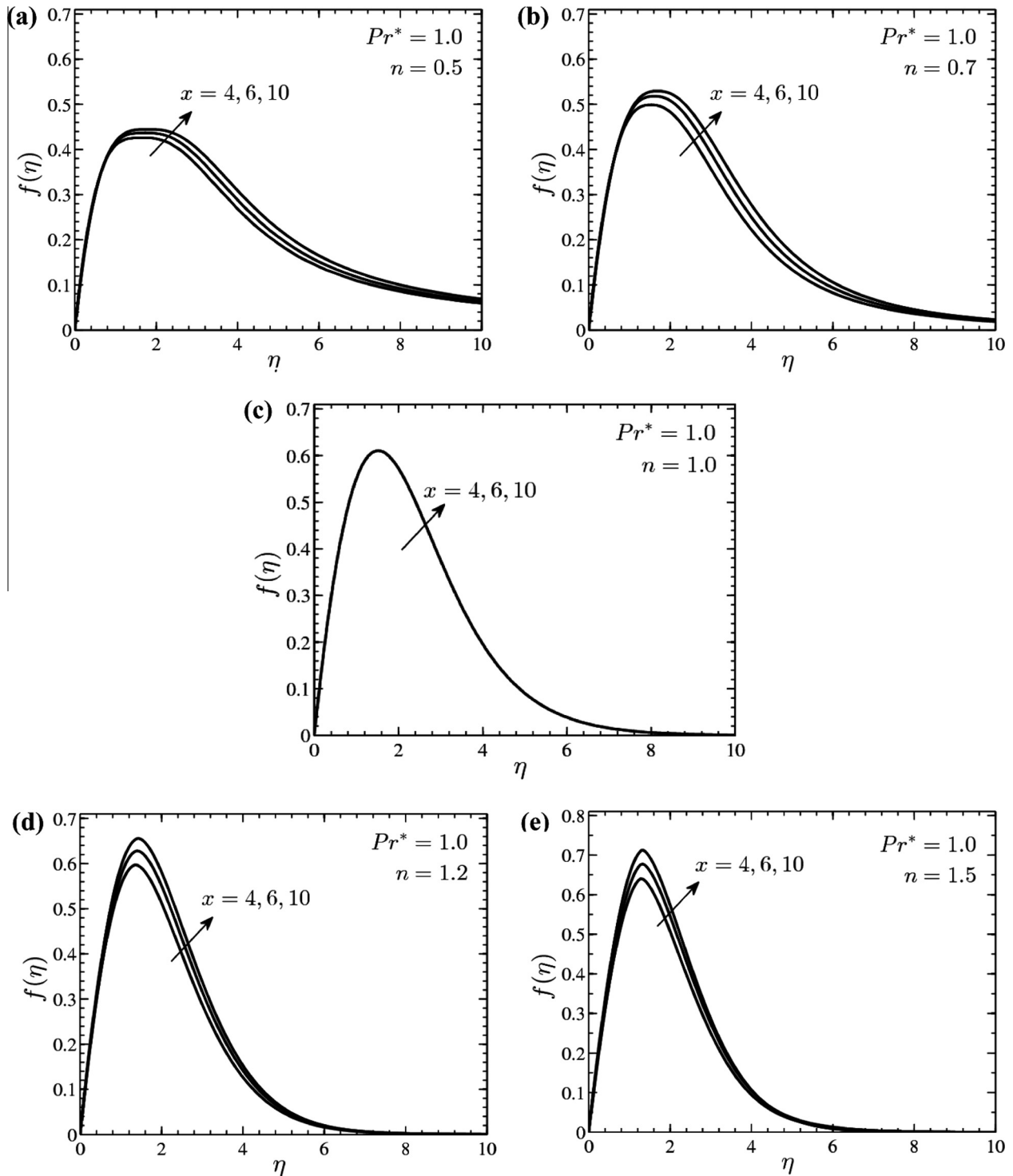


Fig. 7. Non-dimensional u -velocity profiles at different x -locations for $Pr^* = 1$ depicting the non-existence of similarity solution for non-Newtonian fluids ($n \neq 1$). (a) Shear-thinning fluid of $n = 0.5$; (b) shear-thinning fluid of $n = 0.7$; (c) Newtonian fluid $n = 1$; (d) shear-thickening fluid of $n = 1.2$; (e) shear-thickening fluid of $n = 1.5$.

4. Results and discussion

The non-dimensional equations of natural convection boundary layer flow of a Newtonian fluid on isothermal flat plates involve a single parameter – the Prandtl number [13]. In case of non-Newtonian power law fluids this is replaced by the generalised Prandtl number Pr^* which is defined in Eqs. (21) and (22). In addition, another parameter which controls the power-law behaviour of the fluid, called the power-law index (n), appears in the equations.

The generalised Prandtl number reduces to the usual definition of Prandtl number Pr for Newtonian fluids for $n = 1$.

It can be seen in Figs. 2 and 3 that the value of n affects significantly the velocity field but only marginally the temperature field inside the boundary layer for a given Prandtl number Pr^* . As n increases, the maximum \bar{u} -velocity attained at a given x -location increases but the thickness of the velocity boundary layer decreases. Eq. (1) clearly indicates that for $n < 1$ (pseudoplastic or shear-thinning fluids), the effective viscosity increases with decreasing

velocity gradient. For $n > 1$ (dilatant or shear-thickening fluids), the effective viscosity decreases with decreasing velocity gradients. The point where the maximum longitudinal velocity is attained corresponds to a point of zero velocity gradient and consequently a very high effective viscosity for the pseudoplastic fluids. This results in a reduced maximum velocity and the appearance of a near-plateau region in the neighbourhood of this maxima for shear-thinning fluids as compared to Newtonian fluids, both effects increasing with a decrease in n . The reverse happens for dilatant fluids which exhibit higher maximum velocities and sharper peaks as compared to Newtonian fluids. In a natural convective boundary layer flow, the velocity approaches the ambient condition asymptotically at the edge of the boundary layer. This implies that the velocity gradient approaches zero as the boundary layer edge is reached and consequently the effective viscosity increases for $n < 1$. As a consequence, the viscous effects are transmitted up to a greater distance from the plate and the boundary layer is thicker for pseudoplastic fluids as compared to the case of Newtonian fluids. The reverse happens for $n > 1$ and so the boundary layer becomes thinner for shear-thickening fluids.

Fig. 4 shows the variation of the normal component of velocity with varying power-law index n . The \bar{v} -velocity is zero on the surface (no penetration) and attains a constant non-zero value at the edge of the boundary layer. The non-zero value at the boundary layer edge is due to the entrainment of the quiescent fluid resulting in the gradual thickening of the boundary layer along the length of the plate. It is interesting to note that the normal velocity changes sign as we move away from the plate; being positive initially and then negative. It can also be observed in Fig. 4 that the magnitude of the \bar{v} -velocity at the edge of the boundary layer decreases as n increases, which indicates that at the same \bar{x} -location, greater mass of fluid is drawn into the boundary layer for $n < 1$. This is consistent with the occurrence of a thicker boundary layer for $n < 1$ as compared to $n > 1$ as seen in Fig. 2.

In order to visualise the development of the boundary layer for a non-Newtonian power-law fluid, the longitudinal velocity profiles inside the boundary layer at different locations along the plate have been plotted for a dilatant fluid in Fig. 5. This figure tracks the evolution of the velocity profile along the horizontal plate. It can be observed from the figure that, as one moves along the x -direction, the boundary layer thickens and the maximum value of \bar{u} increases. Calculations show that, with increasing \bar{x} , the \bar{y} -location of the maxima in \bar{u} shifts away from the plate. A similar trend of boundary layer development has been observed for the pseudoplastic fluids during the course of present research but the details are not presented here for the sake of brevity.

Fig. 6 shows the spatial variation of pressure inside the boundary layer. The pressure decreases as one traverses along the plate, keeping the \bar{y} -coordinate fixed. Thus, the imposed temperature gradient in the y -direction gives rise to a buoyancy force which, in turn, sets up a pressure gradient in the x -direction such that the natural convective flow becomes possible. This is why such flows were termed as “indirect natural convection” in Section 1. Moreover, pressure also varies with the y -direction such that, at any \bar{x} -location, the minimum pressure occurs at the surface ($\bar{y} = 0$) and the magnitude of this minimum decreases as one moves along the length of the plate. At a particular \bar{x} -location, the pressure increases from the minimum at the surface to reach the ambient condition ($\bar{p} = 0$) asymptotically at the edge of the boundary layer.

The similarity solution for natural convection of a Newtonian fluid over horizontal surfaces has been given in [12,13]. The variables used in the Refs. [12,13] can be recast in terms of the power-law index n as follows:

$$\eta = \frac{\bar{y}}{\bar{x}^{2/(n+4)}}, \quad f(\eta) = \frac{\bar{u}}{\bar{x}^{1/(n+4)}} \tag{40}$$

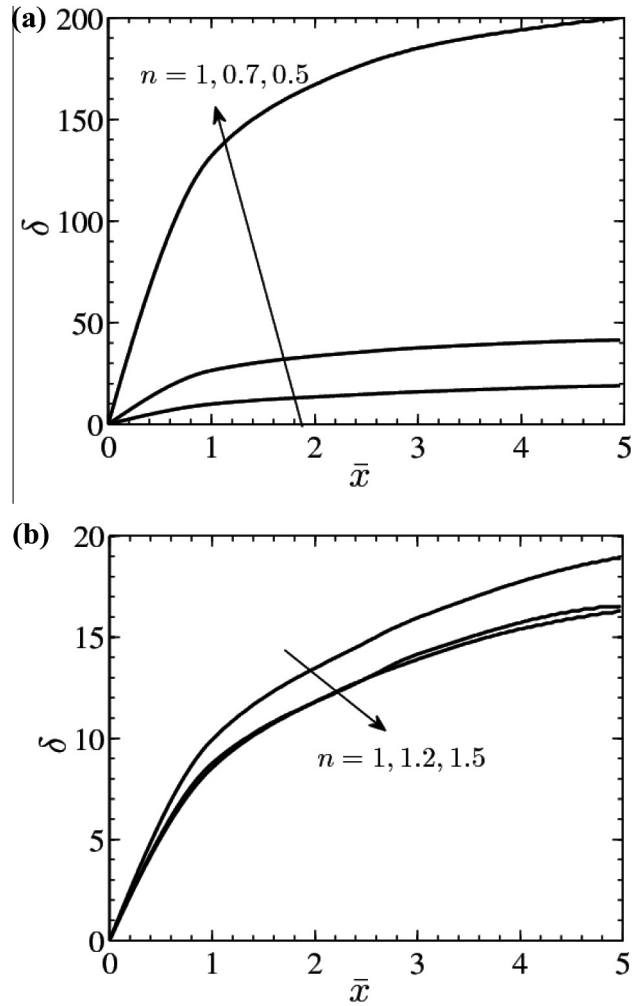


Fig. 8. Growth of the boundary layer along the length of the plate for (a) shear-thinning fluids ($n < 1$); (b) shear-thickening fluids ($n > 1$) in comparison to Newtonian fluid for $Pr^* = 1$. (Notice the different scales along the δ -axis.)

where η is the similarity variable and $f(\eta)$ is the dimensionless longitudinal velocity inside the boundary layer. In order to check the validity of the conclusion reached analytically in Section 2.1, the present computational results, obtained as functions of the two coordinates \bar{x} and \bar{y} , are post-processed and recast in terms of the similarity variables given in Eq. (40); the post-processed results are shown in Fig. 7. The same computer programs are used for all cases (i.e., $n < 1$, $n = 1$ and $n > 1$). For Newtonian fluids ($n = 1$), the plots of $f(\eta)$ versus η at various \bar{x} -locations collapse to a single graph (Fig. 7(c)), as expected (this provides an independent check of the accuracy of the present computer programs). However, Fig. 7(a, b, d and e) shows that in case of a power-law fluid, the plots of $f(\eta)$ versus η at various \bar{x} -locations are not superposed on one another. The maximum deviation in velocity profiles occur near the point of maximum velocity. While the non-similar nature of solutions is mainly observable in the region of maximum velocity for dilatant fluids, pseudoplastics exhibit non-similarity for a greater range of η .

Fig. 7, apart from demonstrating the non-existence of similar solutions, also shows how the quantitative deviation from the Newtonian flow solution depends on how far away from unity the value of n is. A comparison of the five sub-plots of Fig. 7 provides an idea about the rate of deviation from Newtonian behaviour as n is decreased below 1 or increased above 1.

Table 2

Effect of generalised Prandtl number and power-law index on the skin-friction and heat-transfer coefficients.

Pr^*	n	c_f^*	Nu^*
1	0.7	0.7157	0.2032
	1	0.6253	0.2115
	1.2	0.5837	0.2160
5	0.7	0.4333	0.2909
	1	0.3433	0.3161
	1.2	0.3044	0.3295
10	0.7	0.3476	0.3346
	1	0.2651	0.3708
	1.2	0.2304	0.3903

It is interesting to see how the boundary layer thickens as one proceeds along the plate. The thickness of the boundary layer is defined here as the normal distance from the plate at which the non-dimensional streamwise velocity \bar{u} becomes 10^{-4} . Fig. 8 shows that as n increases, the boundary layer thickness decreases. For pseudoplastic fluids (Fig. 8(a)), the boundary layer thickens rapidly over a short distance near the leading edge (much faster than that for Newtonian or dilatant fluids as shown in Fig. 8(b)) and then the rate of growth becomes similar for all values of n (the boundary layer thickness in the pseudoplastic fluids however remains considerably larger than that in Newtonian or dilatant fluids at all values of \bar{x} because of the initial rapid growth). Fig. 8 also shows that if we choose a pseudoplastic and a dilatant fluid such that the value of the power-law index is given by $1 - \epsilon$ and $1 + \epsilon$ respectively, the deviation of boundary layer thickness (from the Newtonian fluid case) will be much more in the case of the pseudoplastic fluid (i.e., $|\delta_{n=1-\epsilon} - \delta_{n=1}| \gg |\delta_{n=1} - \delta_{n=1+\epsilon}|$).

The effect of generalised Prandtl number Pr^* and power-law index n on the reduced skin-friction coefficient c_f^* and reduced Nusselt number Nu^* has been shown in Table 2. It can be seen that as the Prandtl number increases, the skin-friction coefficient decreases but the Nusselt number increases. This finding, which is different from the Reynolds analogy for forced convection, is consistent with the results obtained for natural convection of Newtonian fluids [13].

Table 2 shows that, for a non-Newtonian shear-thickening fluid ($n > 1$), the reduced skin-friction coefficient (c_f^*) is smaller and the reduced Nusselt number (Nu^*) is larger than the corresponding quantities for a Newtonian fluid at the same generalised Prandtl number. Details of the calculation are complex but can be summarized as follows. When $Pr^* \geq 1$, the numerical value of the non-dimensional velocity gradient at the wall $(\partial\bar{u}/\partial\bar{y})_{\bar{y}=0}$ is usually less than unity. It is found that the magnitude of $(\partial\bar{u}/\partial\bar{y})_{\bar{y}=0}$ in fluids with $n > 1$ is greater than the magnitude of $(\partial\bar{u}/\partial\bar{y})_{\bar{y}=0}$ in fluids with $n = 1$. However, when the non-dimensional velocity gradient is raised to the power n (for $n > 1$) in order to calculate c_f^* according to Eq. (27), the value of the reduced skin friction coefficient in the non-Newtonian (dilatant) fluid becomes smaller than that in a Newtonian fluid. The opposite happens for a pseudoplastic ($n < 1$) fluid: the reduced skin-friction coefficient is greater and the reduced Nusselt number is smaller than the corresponding quantities for a Newtonian fluid at the same generalised Prandtl number. It is found that the magnitude of $(\partial\bar{u}/\partial\bar{y})_{\bar{y}=0}$ in fluids with $n < 1$ is smaller than the magnitude of $(\partial\bar{u}/\partial\bar{y})_{\bar{y}=0}$ in fluids with $n = 1$. However, when the non-dimensional velocity gradient (whose numerical value, it is to be remembered, is less than unity for $Pr^* \geq 1$) is raised to the power n (for $n < 1$) in order to calculate (c_f^*) according to Eq. (27), the value of the reduced skin friction coefficient in the non-Newtonian (pseudoplastic) fluid becomes greater than that in a

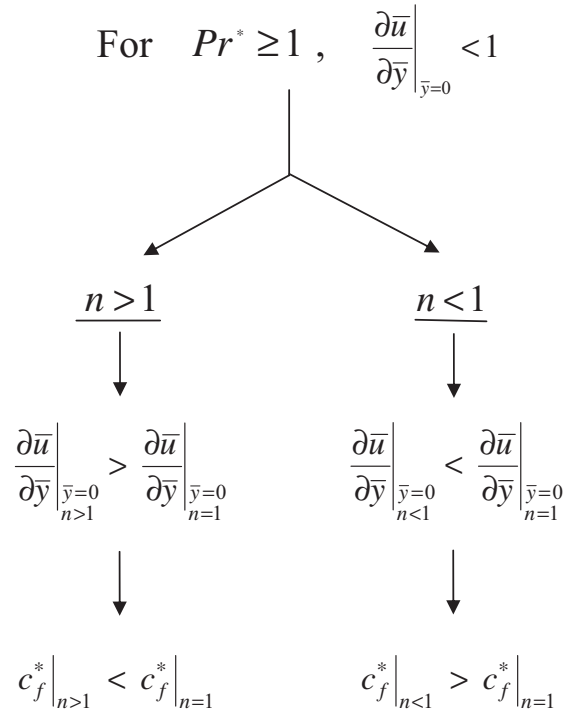


Fig. 9. The values of the reduced skin-friction coefficient for non-Newtonian fluids (shear thinning and thickening) relative to that for Newtonian fluids at a particular Prandtl number.

Newtonian fluid. Fig. 9 summarizes the variation of the reduced skin-friction coefficient with the power-law index n for $Pr^* \geq 1$.

5. Conclusion

A theoretical framework for analysing natural convective boundary layer flow of power-law fluids on horizontal surfaces has been formulated. A robust and generic computational method has been developed that can be implemented to solve natural convection problems where self-similarity does not hold. Example calculations have been performed for five values of n and three values of generalised Prandtl number. An important principle has been established during the present course of computation that, in order to ensure acceptable accuracy of the solution, the size of the computational domain has to be appropriately varied for different values of Pr^* and n such that the flow variables reach the ambient conditions asymptotically.

A few of the important findings from the present work can be summarized as follows.

- It has been shown analytically as well as computationally that self-similarity does not exist if the viscosity shows power-law variation but the thermal conductivity is assumed constant.
- The hydrodynamic boundary layer has been found to be influenced by the non-Newtonian nature of fluid (i.e., by the value of n) while the thermal boundary layer remains almost unaffected for a given generalised Prandtl number.
- The correct scaling velocity for natural convection of non-Newtonian power-law fluids on horizontal surfaces is determined as $u_0 = \frac{\nu_0}{L} (Gr^*)^{(n+1)/(2n+3)}$.
- The maximum \bar{u} -velocity attained within the boundary layer has been found to increase as the value of n increases, while the thickness of the boundary layer decreases with increasing n . As the value of n decreases below 1, a near-plateau region develops in the neighbourhood of the \bar{u} maxima; as the value of n increases above 1, the velocity profile becomes increasingly more peaky.

- The magnitude of the normal velocity component (\bar{v}) at the edge of the boundary layer is found to be smaller for dilatant fluids and greater for pseudoplastic fluids as compared to that of Newtonian fluids.
- For the same Prandtl number, the power-law fluids with $n > 1$ show improved heat transfer characteristics and reduced skin-friction coefficient as compared to the Newtonian fluid.

Appendix Determination of appropriate length and velocity scales in the y -direction

If the length and velocity scales for the boundary layer analysis are chosen as L and u_0 (to be determined), then the non-dimensional variables would be:

$$\bar{x} = \frac{x}{L}, \quad \hat{y} = \frac{y}{L}, \quad \bar{u} = \frac{u}{u_0}, \quad \hat{v} = \frac{v}{u_0}, \quad \theta = \frac{T - T_\infty}{T_w - T_\infty}, \quad (A1)$$

$$\bar{p} = \frac{p - p_\infty}{\rho u_0^2}$$

In Eq. (A1), both x and y coordinates are non-dimensionalized by the length L , but, in reality, a different length scale (δ) arises in the y -direction within a boundary layer. In order not to lose sight of this fact, the notation \hat{y} is used in Eq. (A1). The notation \bar{y} is reserved for a subsequent part of the analysis where the appropriate length scale for the y -direction has been derived and used for the non-dimensionalization. The same comments apply for the variables \hat{v} and \bar{v} .

With the help of non-dimensionalization given in Eq. (A1), the boundary layer equations for a non-Newtonian power-law fluid given as Eqs. (2)–(5) in the main text, can be transformed as follows:

$$\frac{\partial \bar{u}}{\partial \bar{x}} + \frac{\partial \hat{v}}{\partial \hat{y}} = 0 \quad (A2)$$

$$\bar{u} \frac{\partial \bar{u}}{\partial \bar{x}} + \hat{v} \frac{\partial \bar{u}}{\partial \hat{y}} = -\frac{\partial \bar{p}}{\partial \bar{x}} + \frac{1}{Re^*} \frac{\partial}{\partial \hat{y}} \left(\left| \frac{\partial \bar{u}}{\partial \hat{y}} \right|^{n-1} \frac{\partial \bar{u}}{\partial \hat{y}} \right) \quad (A3)$$

$$0 = -\frac{\partial \bar{p}}{\partial \hat{y}} + \frac{Gr^*}{Re^{*2}} \theta \quad (A4)$$

$$\bar{u} \frac{\partial \theta}{\partial \bar{x}} + \hat{v} \frac{\partial \theta}{\partial \hat{y}} = \frac{1}{Re Pr} \frac{\partial^2 \theta}{\partial \hat{y}^2} + \frac{Ec}{Re^*} \left(\frac{\partial \bar{u}}{\partial \hat{y}} \right)^2 \quad (A5)$$

Eq. (A2) implies that if the appropriate velocity scale in the y -direction is v_0 , then v_0/u_0 should be of the same order as δ/L .

The appropriate length scale in the y -direction (δ) can be determined by equating the order of the inertia force with that of the viscous force [13]. This results in,

$$\delta \sim (Re^*)^{-1/(n+1)} \quad (A6)$$

It can be observed in Eq. (A4) that, the term due to buoyancy $\sim O\left(\frac{Gr^*}{Re^{*2}}\right)$ and the term due to pressure gradient $\sim O\left(\frac{1}{\delta}\right)$. Since the pressure gradient in the y -direction is a result of the buoyancy force, they must be of the same order of magnitude. Hence the following relation is obtained:

$$O\left(\frac{Gr^*}{Re^{*2}}\right) \approx O\left(\frac{1}{\delta}\right) \quad (A7)$$

Putting the order of magnitude of the boundary layer thickness from Eq. (A6), and using the definition of Re^* , the scaling velocity to be used for non-dimensionalization is derived to be:

$$u_0 = \frac{v_0}{L} (Gr^*)^{(n+1)/(2n+3)} \quad (A8)$$

Substituting $n = 1$ in the expression for u_0 , the scaling velocity used in case of Newtonian fluids can be ascertained to be $u_0 = \frac{v_0}{L} (Gr)^{2/5}$ which is exactly the same as that given in [13]. The agreement in the limiting case provides a check on the scaling analysis performed here.

Using (A6) and (A7), the dimensionless variables for the normal distance from the plate and normal velocity component are obtained as:

$$\bar{y} = \hat{y} (Gr^*)^{1/(2n+3)}, \quad \bar{v} = \hat{v} (Gr^*)^{1/(2n+3)} \quad (A9)$$

Eq. (A9) provides the basis for the dimensionless variables defined in Eq. (10) in the main text. With the help of these variables, Eqs. (13)–(16) are obtained from Eqs. (A2)–(A5).

References

- [1] A. Florio, A. Harnoy, Combination technique for improving natural convection cooling in electronics, *Int. J. Therm. Sci.* 46 (1) (2007) 76–92.
- [2] K.O. Lim, K.S. Lee, T.H. Song, Primary and secondary instabilities in a glass melting surface, *Numer. Heat Transfer Part A Appl.* 36 (3) (1999) 309–325.
- [3] S. Singh, M.A.R. Sharif, Mixed convective cooling of a rectangular cavity with inlet and exit openings on differentially heated side walls, *Numer. Heat Transfer Part A Appl.* 44 (3) (2003) 233–253.
- [4] P.M. Patil, P.S. Kulkarni, Effects of chemical reaction on free convective flow of a polar fluid through a porous medium in the presence of internal heat generation, *Int. J. Therm. Sci.* 47 (8) (2008) 1043–1054.
- [5] A. Som, J.L.S. Chen, Free convection of non-Newtonian fluids over non-isothermal two-dimensional bodies, *Int. J. Heat Mass Transfer* 27 (5) (1984) 791–794.
- [6] Z.P. Shulman, Z.I. Baikov, E.A. Zaltsgendler, An approach to prediction of free convection in non-Newtonian fluids, *Int. J. Heat Mass Transfer* 19 (9) (1976) 1003–1007.
- [7] Z.U.A. Warsi, Unsteady flow of power-law fluids through circular pipes, *J. Non-Newtonian Fluid Mech.* 55 (2) (1994) 197–202.
- [8] R.P. Chhabra, J.F. Richardson, *Non-Newtonian Flow and Applied Rheology Engineering Applications*, second ed., Butterworth-Heinemann, UK, 2008.
- [9] L.C. Burmeister, *Convective Heat Transfer*, second ed., John Wiley and Sons, New York, 1993.
- [10] H. Schlichting, K. Gersten, *Boundary Layer Theory*, Springer, New Delhi, 2004.
- [11] K. Stewartson, On the free convection from a horizontal plate, *Z. Angew. Math. Phys. (ZAMP)* 9 (3) (1958) 276–282.
- [12] Z. Rotem, L. Claassen, Natural convection above unconfined horizontal surfaces, *J. Fluid Mech.* 39 (1) (1969) 173–192.
- [13] S. Samanta, A. Guha, A similarity theory for natural convection from a horizontal plate for prescribed heat flux or wall temperature, *Int. J. Heat Mass Transfer* 55 (13–14) (2012) 3857–3868.
- [14] A. Acrivos, A theoretical analysis of laminar natural convection heat transfer to non-Newtonian fluids, *AIChE J.* 6 (4) (1960) 584–590.
- [15] C.C. Gentry, D.E. Wollersheim, Local free convection to non-Newtonian fluids from a horizontal isothermal cylinder, *J. Heat Transfer* 96 (1) (1974) 3–8.
- [16] M.L. Ng, J.P. Hartnett, Free convection heat transfer from horizontal wires to pseudoplastic fluids, *Int. J. Heat Mass Transfer* 31 (2) (1988) 441–447.
- [17] A.V. Shenoy, R.A. Mashelkar, Thermal convection in non-Newtonian fluids, *Adv. Heat Transfer* 15 (1982) 143–225.
- [18] M.J. Huang, C.K. Chen, Local similarity solutions of free convective heat transfer from a vertical plate to non-Newtonian power-law fluids, *Int. J. Heat Mass Transfer* 33 (1) (1990) 119–125.
- [19] S. Ghosh Moulic, L.S. Yao, Non-Newtonian natural convection along a vertical flat plate with uniform surface temperature, *J. Heat Transfer* 131 (6) (2009) 1–8.
- [20] A.J. Chamkha, A.M. Aly, M.A. Mansour, Unsteady natural convective power-law fluid flow past a vertical plate embedded in a non-Darcian porous medium in the presence of a homogeneous chemical reaction, *Nonlinear Anal. Modell. Control* 15 (2) (2010) 139–154.
- [21] T.-Y. Wang, Mixed convection heat transfer from a horizontal plate to non-Newtonian fluids, *Int. Commun. Heat Mass Transfer* 20 (6) (1993) 845–857.